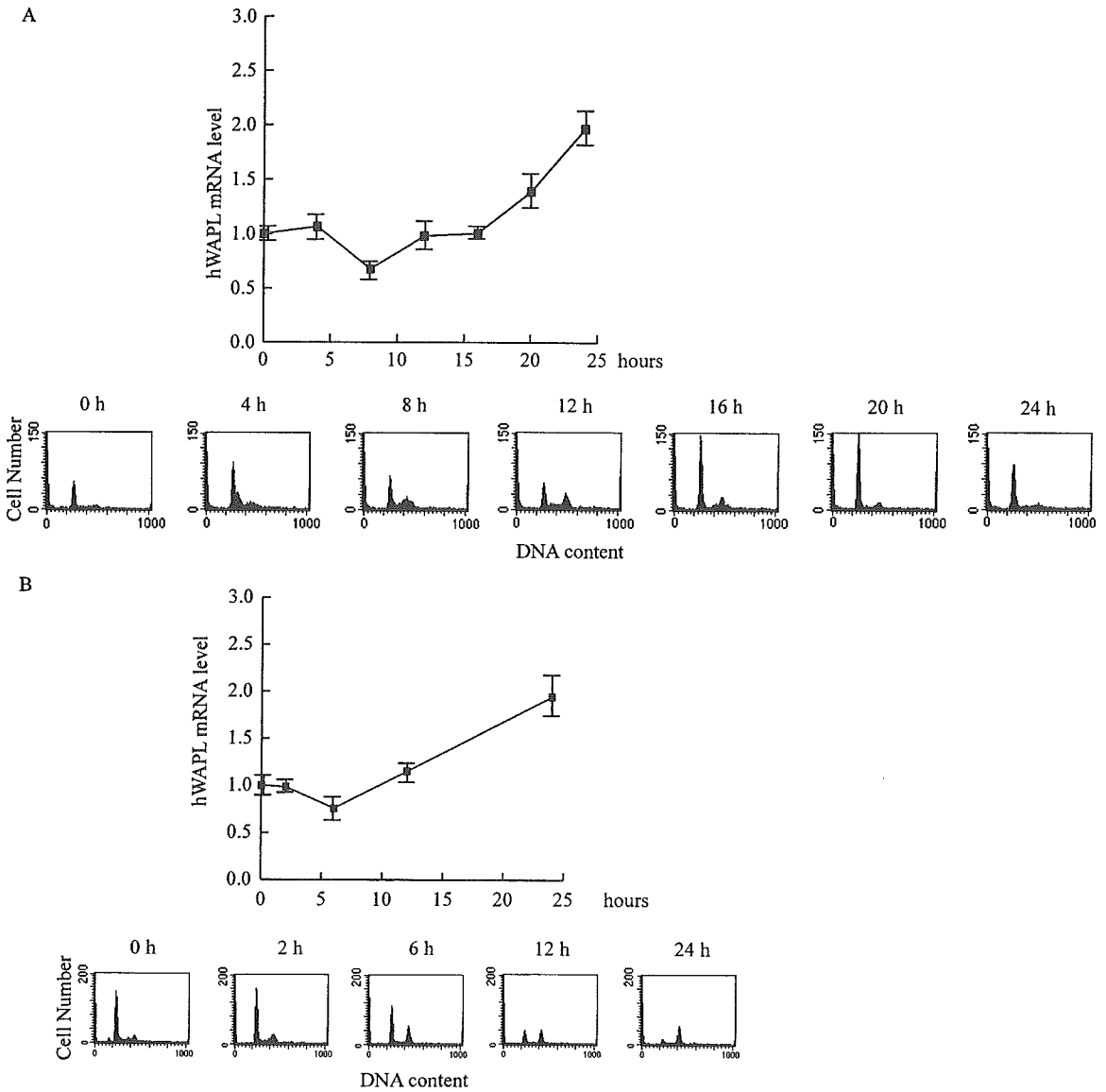

Fig. 3. Cell cycle profiles and *hWAPL* mRNA levels. *hWAPL* mRNA levels in the cells were determined by real time PCR analysis. Data were normalized to the mRNA level at 0 h that was arbitrarily set to 1 in the graphical presentation. *Bars, s.e.*. Cell cycle profiles of the cells at each time points were also confirmed by flow cytometric analysis. (A) Kinetics of *hWAPL* mRNA levels in SiHa cells at 0, 4, 8, 12, 16, 20 and 24 h after releasing from G1 arrest by 1 μg/ml aphidicolin treatment. (B) Kinetics of *hWAPL* mRNA levels in SiHa cells at 0, 2, 6, 12 and 24 h after 50 ng/ml nocodazole treatment.

3. Results and discussion

To examine whether 3-MC affects *hWAPL* expression, we treated various human uterine cervical cancer-derived cell lines with dimethylsulfoxide (DMSO) alone or 3-MC for 6 h. Then, we calculated the amounts of the *hWAPL* mRNAs in the cells by quantitative real time PCR analysis, and found that *hWAPL* mRNA levels were increased in the 3-MC-treated cells (Fig. 1A). The increases in *hWAPL* mRNA levels in SiHa cells was most remarkable among the cell lines examined. Because the *CYP1A1* gene is

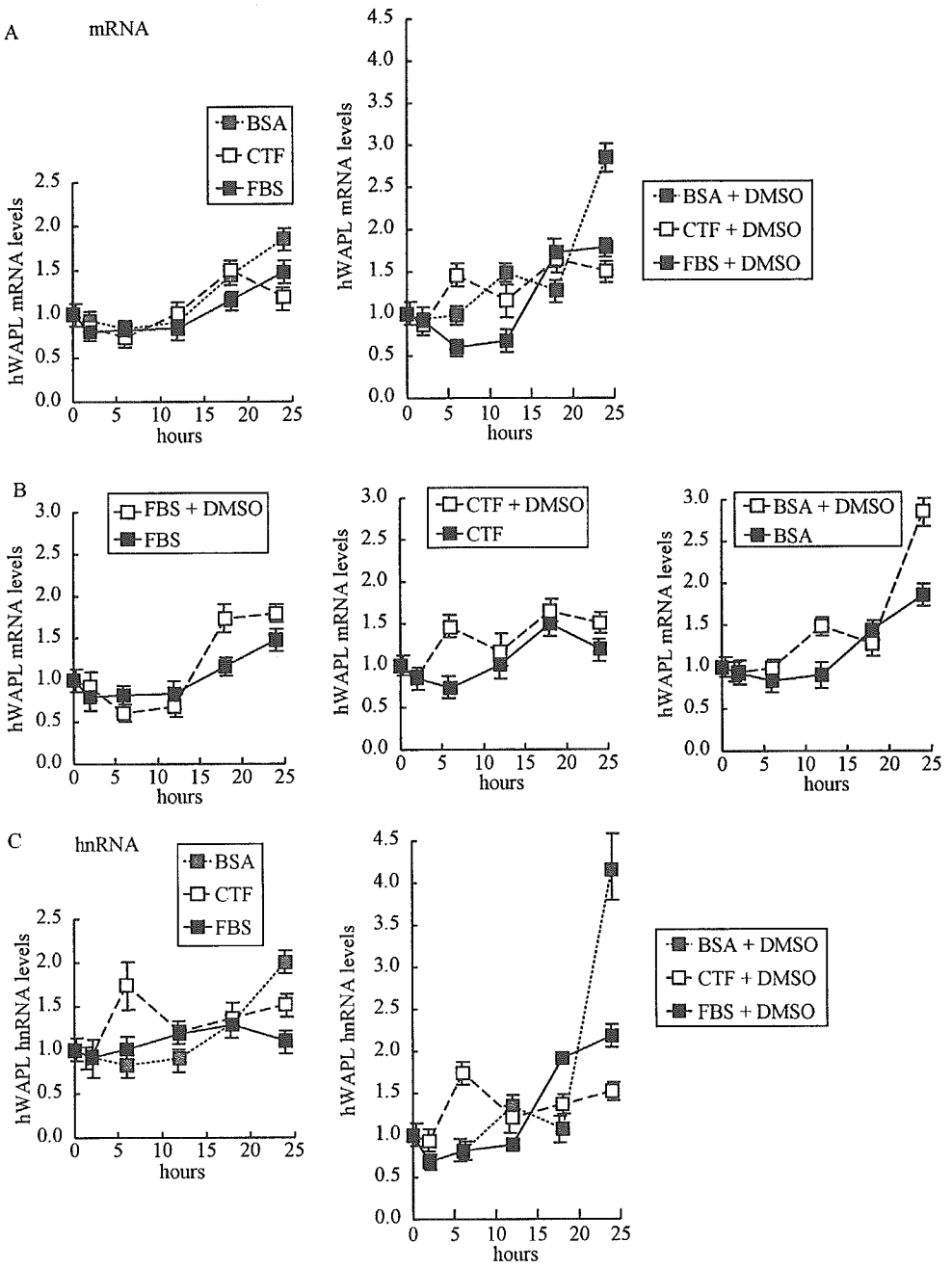

Fig. 4. Effects of FBS, CTF, BSA and DMSO on *hWAPL* mRNA and hnRNA levels in SiHa cells. *hWAPL* mRNA and hnRNA levels in SiHa cells at 0, 2, 6, 12, 18 and 24 h after replacing the growth medium to a fresh medium supplemented with FBS, CTF or BSA with or without 0.1% DMSO were deteremined by real time PCR analysis. Data were normalized to the mRNA and hnRNA level at 0 h that was arbitrarily set to 1 in the graphical presentation. *Bars, s.e.* (A) Kinetics of the *hWAPL* mRNA levels in the cells grown in the growth medium supplemented as indicated. (B) Graphical representation of the effects of DMSO on the kinetics of *hWAPL* mRNA levels in the cells grown in the growth medium supplemented with FBS, CTF or BSA. (C) Kinetics of the *hWAPL* hnRNA levels in the cells grown in the growth medium supplemented as indicated.

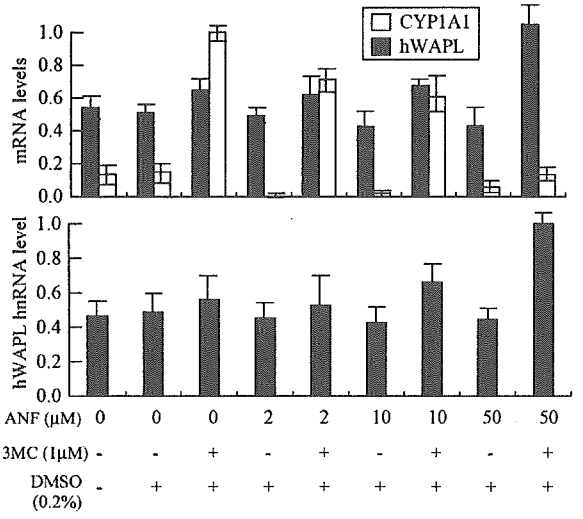

Fig. 5. Effects of AhR inhibition by α-naphthoflavone on *hWAPL* mRNA and hnRNA levels in SiHa cells treated with 3-MC. SiHa cells were treated with 0.2% DMSO alone or 1 μM 3-MC with 0. 2, 10 or 50 μM ANF for 6 h. Then, the *hWAPL* mRNA and hnRNA levels and the *CYP1A1* mRNA levels were deteremined by real time PCR analysis. SiHa cells grown for 6 h in a normal fresh medium without chemicals were also analyzed as a normal control. Data were normalized to the maximaum mRNA and hnRNA levels that were arbitrarily set to 1 in the graphical presentation. *Bars, s.e.*

a well-known target of 3-MC [12,13], we also calculated *CYP1A1* mRNA levels in the three cell lines to confirm the effects of 3-MC on the cells (Fig. 1A). We found that *CYP1A1* mRNA levels in SiHa cells were highest and increased most remarkable. *CYP1A1* mRNA in CaSki cells was not detected in our experiments. We also observed that hWAPL protein level was increased in the 3-MC-treated SiHa cells (Fig. 1B).

We next examined the effects of 3-MC on *hWAPL* expression in SiHa cells at several time points after 3-MC treatment (Fig. 2). The 3-MC-treated cells showed higher levels of *hWAPL* mRNA than the control cells at all time points examined. Interestingly, the *hWAPL* mRNA levels decreased first 6 h and then increased after changing the medium to a fresh medium containing DMSO with or without 3-MC as seen in Fig. 2.

These results prompted us to investigate whether the *hWAPL* expression is related to the cell cycle. First, to synchronize cell cycle progression, we treated SiHa cells with aphidicolin, an inhibitor of DNA synthesis, for 12 h to induce G1-phase arrest. We then released the cells from G1 arrest by changing the culture medium to a fresh growth medium. The synchronized cells were harvested every 4 h for 24 h after release from aphidicolin, and the *hWAPL* mRNA levels were calculated by quantitative real time PCR analysis (Fig. 3A). As seen in Fig. 3A, *hWAPL* mRNA initially decreased and then increased over time. Flow cytometric analysis confirmed the cell cycle phase of the cells at each time point (Fig. 3A). From these results, *hWAPL* mRNA level seemed to fluctuate in accordance with cell cycle profile. However, the levels of *hWAPL* mRNA in the cells treated with nocodazole, an inhibitor of spindle assembly, fluctuated in a similar manner to the aphidicolin-synchronized cells (Fig. 3B). Thus, amounts of *hWAPL* mRNAs are likely to have no relation to the cell cycle profiles. Recently, Guigal et al. demonstrated that FBS induces transcription of the *CYP1A1* gene. Therefore, we suspected that the fluctuation of *hWAPL* mRNA levels might be associated with the culture medium change.

To investigate the effects of components in FBS on the fluctuation of *hWAPL* mRNA levels, we examined the *hWAPL* mRNA levels in SiHa cells after changing growth medium to a fresh medium supplemented with charcoal/dextran treated FBS (CTF) or BSA instead of FBS. The fluctuations of the *hWAPL* mRNA levels showed similar trends among the cells grown with FBS, CTF and BSA (Fig. 4A; left panel). However, all cells examined in Figs. 1–3 were grown in the medium containing DMSO. Thus, we also tested the effects of DMSO with FBS, CTF or BSA at the same time. Interestingly, fluctuations of the *hWAPL* mRNA levels in SiHa cells treated with 0.1% DMSO showed different trends among FBS, CTF and BSA (Fig. 4A; right panel), and the *hWAPL* mRNA levels in the DMSO-treated cells fluctuated more drastically than that in the cells grown without DMSO (Fig. 4B). Especially, remarkable decrease of *hWAPL* mRNA levels for first 6 h after the medium change was distinctive for the growth medium supplemented with FBS and DMSO. These results suggest that DMSO and some constituents of FBS affect *hWAPL* mRNA accumulation synergistically.

mRNA levels do not always reflect on the transcription activity of genes. To investigate the kinetics of the promoter activities of the *hWAPL* gene in the cells, we evaluated the levels of *hWAPL* heterogeneous nuclear RNA (hnRNA), the unprocessed precursor of the mature and functional mRNA,

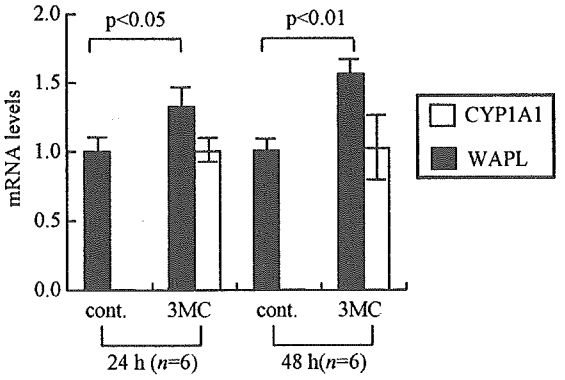

Fig. 6. Effects of 3-MC on *WAPL* mRNA levels in mouse uteri. The mice received a single intraperitoneal injection of 1 ml of olive oil containing 3-MC (3-MC) or olive oil only (cont.), and *WAPL* mRNA levels in the uteri at 24 and 48 h after injection were determined with quantitative real time PCR analysis. *CYP1A1* mRNA levels were also deteremined to confirm the effects of 3-MC on mouse uteri. The data represent the means of multiple samples normalized to the mean values of the *hWAPL* mRNA levels in the cont. 24 h samples and *CYP1A1* mRNA levels in the 3-MC 24 h samples, respectively, that were arbitrarily set to 1 in the graphical presentation. *Bars, s.e.*

by real time PCR using intron-specific primers for *hWAPL* searched in Ensembl Genome Browser (http://www.ensembl.org/). Levels of hnRNA have been proposed as a surrogate for nuclear run-on assays to determine gene transcription rates [14,15]. Although the *hWAPL* hnRNA levels fluctuated in somewhat different manner to the mRNA levels in the cells grown without DMSO, the *hWAPL* hnRNA levels in the DMSO-treated cells fluctuated in similar manner to the mRNA levels (Fig. 4C; compare with Fig. 4A). These results suggest that DMSO and some components of FBS affect transcriptional activity of the *hWAPL* gene. Increase of *hWAPL* transcription levels at 24 h in common with the cells under various conditions may be caused by the accumulation of wastes in their growth medium.

3-MC is known to be an agonist of AhR [16]. Thus, to investigate whether AhR is related to *hWAPL* transcription activation, we examined the effects of α-naphthoflavone (ANF), an AhR antagonist [17], at a dose of 2, 10 and 50 μM on *hWAPL* mRNA and hnRNA levels in 3-MC-treated SiHa cells by quantitative real time PCR analysis (Fig. 5). We also evaluated *CYP1A1* mRNA levels for monitoring the inhibitory effects on AhR functions by ANF, and found that 50 μM of ANF strongly inhibited AhR functions (Fig. 5; upper panel). Interestingly, increase of *hWAPL* mRNA levels by 3-MC was more remarkable in AhR-inhibited cells rather than that in AhR-functioning normal cells. Induction of *hWAPL* hnRNA levels showed similar manner to the *hWAPL* mRNA (Fig. 5; lower panel). From these results, we hypothesized that AhR was involved in the transcriptional regulation of *hWAPL*, but there are complex mechanisms for the transcriptional regulation of *hWAPL*. We did not find XRE motif in 5000 bp of 5′-upstream sequence of the *hWAPL* gene using MOTIF Sequence Motif Search (http://motif.genome.jp/) at the cut off score 85. Thus, although further investigation is required, we suppose that *hWAPL* is not a direct target of 3-MC but a down stream molecule of a 3-MC-targeted molecule.

Finally, we examined whether the mRNA level of a mouse homolog of *hWAPL* is increased by 3-MC in mouse uterus. Twenty-four and 48 h after the injection of 3-MC into the abdominal cavities of C57/BL6 female mice, we harvested the uteri and analyzed the *WAPL* mRNA levels by quantitative real time PCR analysis. The *CYP1A1* mRNA levels were also analyzed to confirm the 3-MC effects on the uteri. The uteri exhibited increases in *WAPL* mRNA levels compared with that of control mice (Fig. 6). These data suggest that 3-MC exposure affects *WAPL* expression in uterus.

Our recent data demonstrated that the unscheduled increase of *hWAPL* expression in human uterine cervix is associated with cervical cancer [1]. In Addition, previous studies demonstrated that 3-MC induces carcinogenesis in mouse uterine cervix [18, 19]. Thus, although the *hWAPL* induction by 3-MC was weak in our experiments, our results suggest that the promotion of carcinogenesis by 3-MC in uterus is likely to involve the *hWAPL* oncogene.

Acknowledgements

This work was supported by a Grant-in-Aid for scientific research on Priority Area (C) from the Ministry of Education, Science, Sports and Culture, and a grant from Core Research for Evolutional Science and Technology (CREST), Japan Science and Technology Corporation.

References

[1] K. Oikawa, T. Ohbayashi, T. Kiyono, H. Nishi, K. Isaka, A. Umezawa, et al., Expression of a novel human gene, human wings apart-like (hWAPL), is associated with cervical carcinogenesis and tumor progression, Cancer Res. 64 (2004) 3545–3549.

[2] F. Verni, R. Gandhi, M.L. Goldberg, M. Gatti, Genetic and molecular analysis of wings apart-like (wapl), a gene controlling heterochromatin organization in *Drosophila melanogaster*, Genetics 154 (2000) 1693–1710.

[3] K.W. Dobie, C.D. Kennedy, V.M. Velasco, T.L. McGrath, J. Weko, R.W. Patterson, G.H. Karpen, Identification of chromosome inheritance modifiers in *Drosophila melanogaster*, Genetics 157 (2001) 1623–1637.

[4] S. Reynaud, C. Duchiron, P. Deschaux, 3-Methylcholanthrene increases phorbol 12-myristate 13-acetate-induced respiratory burst activity and intracellular calcium levels in common carp (Cyprinus carpio L) macrophages, Toxicol. Appl. Pharmacol. 175 (2001) 1–9.

[5] J. Mimura, Y. Fujii-Kuriyama, Functional role of AhR in the expression of toxic effects by TCDD, Biochim. Biophys. Acta 1619 (2003) 263–268.

[6] K. Sogawa, Y. Fujii-Kuriyama, Ah receptor, a novel ligand-activated transcription factor, J. Biochem. (Tokyo) 122 (1997) 1075–1079.

[7] K. Oikawa, T. Ohbayashi, J. Mimura, R. Iwata, A. Kameta, K. Evine, et al., Dioxin suppresses the checkpoint protein, MAD2, by an aryl hydrocarbon receptor-independent pathway, Cancer Res. 61 (2001) 5707–5709.

[8] S.R. Kondraganti, P. Fernandez-Saluguero, F.J. Gonzalez, K.S. Ramos, W. Jiang, B. Moorthy, Polycyclic aromatic hydrocarbon-inducible DNA adducts: evidence by 32P-postlabeling and use of knockout mice for Ah receptor-independent mechanisms of metabolic activation in vivo, Int. J. Cancer 103 (2003) 5–11.

[9] K. Oikawa, T. Ohbayashi, J. Mimura, Y. Fujii-Kuriyama, S. Teshima, K. Rokutan, et al., Dioxin stimulates synthesis and secretion of IgE-dependent histamine-releasing factor, Biochem. Biophys. Res. Commun. 290 (2002) 984–987.

[10] M. Kuroda, T. Ishida, M. Takanashi, M. Satoh, R. Machinami, T. Watanabe, Oncogenic transformation and inhibition of adipocytic conversion of preadipocytes by TLS/FUS-CHOP type II chimeric protein, Am. J. Pathol. 151 (1997) 735–744.

[11] K. Oikawa, Y. Kosugi, T. Ohbayashi, A. Kameta, K. Isaka, M. Takayama, et al., Increased expression of IgE-dependent histamine-releasing factor in endometriotic implants, J. Pathol. 199 (2003) 318–323.

[12] N. Guigal, E. Seree, V. Bourgarel-Rey, Y. Barra, Induction of CYP1A1 by serum independent of AhR pathway, Biochem. Biophys. Res. Commun. 267 (2000) 572–576.

[13] N. Guigal, E. Seree, Q.B. Nguyen, B. Charvet, A. Desobry, Y. Barra, Serum induces a transcriptional activation of CYP1A1 gene in HepG2 independently of the AhR pathway, Life Sci. 68 (2001) 2141–2150.

[14] C.J. Elferink, J.J. Reiners Jr., Quantitative RT-PCR on CYP1A1 heterogeneous nuclear RNA: a surrogate for the in vitro transcription run-on assay, Biotechniques 20 (1996) 470–477.

[15] R.F. Johnson, C.M. Mitchell, W.B. Giles, W.A. Walters, T. Zakar, The in vivo control of prostaglandin H synthase-2 messenger ribonucleic acid expression in the human amnion at parturition, J. Clin. Endocrinol. Metab. 87 (2002) 2816–2823.

[16] M. Naruse, Y. Ishihara, S. Miyagawa-Tomita, A. Koyama, H. Hagiwara, 3-Methylcholanthrene, which binds to the arylhydrocarbon receptor, inhibits proliferation and differentiation of osteoblasts in vitro and ossification in vivo, Endocrinology 143 (2002) 3575–3581.

[17] T.A. Gasiewicz, G. Rucci, Alpha-naphthoflavone acts as an antagonist of 2,3,7, 8-tetrachlorodibenzo-p-dioxin by forming an inactive complex with the Ah receptor, Mol. Pharmacol. 40 (1991) 607–612.

[18] P. Das, A.R. Rao, P.N. Srivastava, Influence of ascorbic acid on MCA-induced carcinogenesis in the uterine cervix of mice, Cancer Lett. 72 (1993) 121–125.

[19] S. Gagandeep, S. Dhanalakshmi, E. Mendiz, A.R. Rao, R.K. Kale, Chemopreventive effects of Cuminum cyminum in chemically induced forestomach and uterine cervix tumors in murine model systems, Nutr. Cancer 47 (2003) 171–180.

Neuropathology 2005; **25**, 263–268

Workshop: Modern techniques for the pathological investigation of brain tumors

Detection of fusion genes in sarcomas using paraffin-embedded tissues

Keiichi Yoshida, Kosuke Oikawa, Masakatsu Takanashi and Masahiko Kuroda

Department of Pathology, Tokyo Medical University, Tokyo, Japan

Many sarcomas are characterized by specific recurrent chromosomal translocations resulting in gene fusions. The genes involved in almost all of these translocations have been cloned, greatly changing sarcoma diagnosis. At the biological level, these chromosomal translocations produce highly specific fusion genes that encode key molecules for tumor development. The clinical correlation between these translocation-derived genetic markers and discrete histopathological entities has been remarkable. Today, detection of fusion genes plays a crucial role in the diagnosis of sarcomas that harbor atypical clinical or pathological presentations. The focus of this brief review is the recent impact that cytogenetic and molecular detection of these translocations has had on sarcoma diagnosis using paraffin-embedded sections.

Key words: fluorescence *in situ* hybridization, fusion genes, paraffin-embedded tissues, reverse transcription-polymerase chain reaction, sarcomas.

INTRODUCTION

Some sarcomas are characterized by specific translocations resulting in gene fusions, and the resulting genetic lesions now constitute very powerful diagnostic markers.[1–3] Most of these gene fusions are listed in Table 1. These tumor markers are particularly useful for the precise diagnosis of sarcomas and small round cell tumors of children and young adults, which sometimes harbor atypical clinical or pathological presentations.

Interestingly, these fusion genes usually encode aberrant chimeric transcription factors, and their gene products show transformation activity. In addition, recent research revealed crucial downstream molecules of the chimeric transcription factors (Table 1).[4–29] These discoveries have provided important signposts for the pathogenesis of specific sarcomas.

Identification of such specific chromosomal translocations or fusion genes known to characterize particular tumors can facilitate tumor diagnoses and provide a prognostic implication. The cytogenetic and molecular approaches to detect these translocations or rearranged genes usually require fresh or snap-frozen samples of tissues or cultured cells. Because these materials are not always available, methods applicable to paraffin-embedded samples are necessary to identify such translocations or gene rearrangements for diagnostic and prognostic purposes. Thus far, nested reverse transcription-polymerase chain reaction (RT-PCR) has been a major tool for the detection of these molecular or genetic alterations in tumors, using paraffin-embedded tissues.

METHODS FOR THE DETECTION OF FUSION GENES USING PARAFFIN-EMBEDDED SECTIONS

Reverse transcription-polymerase chain reaction

The breakpoints of chromosomal translocations occur within introns but not exons. By chromosomal translocation, these introns – on separate chromosomes – are fused and translated as a part of a novel chimeric gene. Thus, RT-PCR is a standard method for the specific detection of chimeric RNA transcripts resulting from these chromosomal translocations. In general, the detection of these translocations or rearranged genes for diagnostic and prognostic purposes requires fresh or snap-frozen samples of tumor tissues, or cultured tumor cells. Fresh or snap-frozen materials are not always available, however, and, thus, methods suitable for paraffin-embedded samples are often required. Indeed, RT-PCR is a reliable and sensitive technique for the analysis of tumor samples from paraffin sections.

Correspondence: Masahiko Kuroda, MD, Department of Pathology, Tokyo Medical University, 6-1-1 Shinjuku, Shinjuku-ku, Tokyo 160-8402, Japan. Email: kuroda@tokyo-med.ac.jp

Received 13 April 2005; accepted 18 April 2005.

Table 1 Gene fusions in soft tissue tumors

Tumor type	Translocation	Fusion transcript	Putative function of fusion transcipt products	Reference
PNET/Ewing's sarcoma	t(11;22)(q24;q12)	*EWS-FLI1*	ETS-like DNA binding	4
	t(21;22)(q22;q12)	*EWS-ERG*	Gln-Ser-Try/Gly-rich/RNA binding ETS-like DNA binding	5,6
	t(7;22)(p22;q12)	*EWS-ETV1*	Gln-Ser-Try/Gly-rich/RNA binding ETS-like DNA binding	7
	t(9;22)(q12;q12)	*EWS-E1A-F*	Gln-Ser-Try/Gly-rich/RNA binding DNA binding (adenovirus E1A enhancer-binding)	8,9
	t(2;22)(q33;q12)	*EWS-FEV*	Gln-Ser-Try/Gly-rich/RNA binding ETS-like DNA binding	10
Clear cell sarcoma	t(12;22)(q13;q12)	*EWS-ATF1*	Gln-Ser-Try/Gly-rich/RNA binding bZIP DNA binding	11
Desmoplastic small round cell tumor	t(11;22)(p13;q12)	*EWS-WT1*	Gln-Ser-Try/Gly-rich/RNA binding DNA binding	12
Extraskeletal myxoid chondrosarcoma	t(9;22)(q22;q12)	*EWS-CHN*	Gln-Ser-Try/Gly-rich/RNA binding DNA binding	13,14
	t(9;17)(q22;q11)	*TAFII68/RBP56-CHN*	Gln-Ser-Try/Gly-rich/RNA binding DNA binding	15–17
Alveolar rhabdomyosarcoma	t(2;13)(q35;q14)	*FKHR-PAX3*	Gln-Ser-Try/Gly-rich/RNA binding Paired box/homeodomain	18,19
	t(1;13)(p36;q14)	*FKHR-PAX7*	Forkhead DNA binding Paired box/homeodomain	20
Myxoid liposarcoma	t(12;16)(q13;p11)	*TLS/FUS-CHOP*	Forkhead DNA binding DNA binding/ZIP	21,22
	t(12;22)(q12;q13)	*EWS-CHOP*	Gln-Ser-Try/Gly-rich/RNA binding DNA binding/ZIP	23
Synovial sarcoma	t(X;18)(p11;q11)	*SYT-SSX1*	Gln-Ser-Try/Gly-rich/RNA binding Kruppel-associated box/None identified	24
	t(X;18)(p11;q11)	*SYT-SSX2*	None identified Kruppel-associated box/None identified	25,26
	t(X;18)(p11;q11)	*SYT-SSX4*	None identified Kruppel-associated box/None identified	27
Dermatofibrosarcoma protuberans	t(17;12)(q22;q13)	*COLIA1-PDGFB*	None identified Extracellular matrix Growth factor	28
Congenital/infantile fibrosarcoma	t(12;15)(p13;q25)	*ETV6-NTRK3*	Helix-loop-helix protein Tyrosine kinase receptors	29

PNET, peripheral neuroectodermal tumor.

Fluorescence *in situ* hybridization

Interface fluorescence *in situ* hybridization (FISH), optimally performed on cell suspensions or cytological touch preparations of fresh or frozen tumors, is adaptable to paraffin-embedded tissue samples and is a rapid and effective alternative to RT-PCR.[30–37] In addition, *in situ* hybridization is the only technique that provides the localization of cells carrying a chimeric gene in a heterogeneous cell population.

Chromosomes are not randomly arranged within the interphase nuclei of plant and animal cells; each chromosome occupies its own distinct region called a "territory".[38] Recently, we examined the relative and radial 3-D positioning of the chromosome territories of human chromosomes 12 and 16 during adipocyte differentiation (Fig. 1A,B), and detected a close association between the territories in differentiated adipocytes (Fig. 1B).[39] This association of chromosomes 12 and 16 may facilitate the translocation between chromosomes 12 and 16. However, two methods are used for the detection of translocations using dual-colored dyes (Fig. 2A,B). One method uses the two probes hybridized to the genomic regions positioned on opposite sides from the breakpoint on a single translocated chromosome. The other method uses the two probes hybridized to regions on separate chromosomes. The latter method (Fig. 2B) might recognize normal cells as tumor cells if the positions of the two chromosomes are very close, as in adipocytes. Thus, the positions of the probes must be carefully determined.

Immunohistochemistry

Some fusion proteins resulting from these translocations may be demonstrable immunohistochemically, taking advantage of three aspects of their biology. First, fusion proteins induce overexpression of a target protein that may not normally be expressed in this type of tissue. For example, the fusion oncoproteins TLS-CHOP and EWS-CHOP are characteristic markers for myxoid and round cell liposarcomas. DOL54 is inducible by TLS-CHOP and EWS-CHOP, but not by TLS, EWS, or CHOP.[40] Therefore, DOL54 expression is a helpful diagnostic marker for myxoid liposarcoma. Second, only the amino- or carboxyl-terminal portion of a given protein may be expressed. Third, an exon not usually translated may be translated when translocation occurs. For instance, in the case of myxoid liposarcoma, the peptide sequence of 26 amino acids corresponding to the normally untranslated *CHOP* exon 2 and parts of exon 3 (5'-UTR) is a unique structure of these chimeric proteins. Antibodies[41] against the specific regions of the fusion protein are potentially useful in the immunocytochemical detection of TLS-CHOP. Although this type of approach depends on the structure of the fusion genes, immunohistochemistry is very useful if specific antibodies are available.

MOLECULAR DIAGNOSIS IN ARCHIVAL PATHOLOGY MATERIAL

RNA in paraffin-embedded sections

As mentioned previously, one of the most reliable techniques for the detection of fusion genes in formalin-fixed, paraffin-embedded archival pathology materials is RT-PCR. Recent technical refinements have made it more feasible; however, RNA in the formalin-fixed, paraffin-embedded materials are degraded to sizes often less than 300 bp. Thus, in order to obtain RNA of sufficient quality

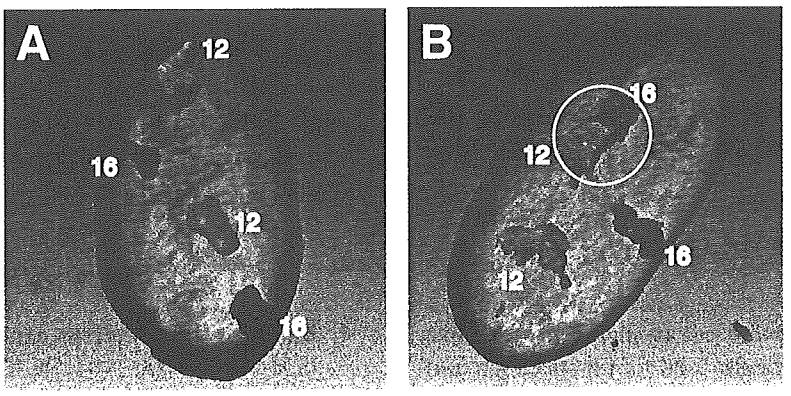

Green, CT12; Red, CT16; Blue, Nucleus.

Fig. 1 Three-dimensional positioning of chromosome 12 (green) and chromosome 16 (red) (CT12 and CT16, respectively) in a (A) human preadipocyte nucleus and (B) human adipocyte nucleus. Note that the adipocyte nucleus displays a proximal association of one CT12 and one CT16 (B), whereas the preadipocyte nucleus shows no association between CT12 and CT16 (A).

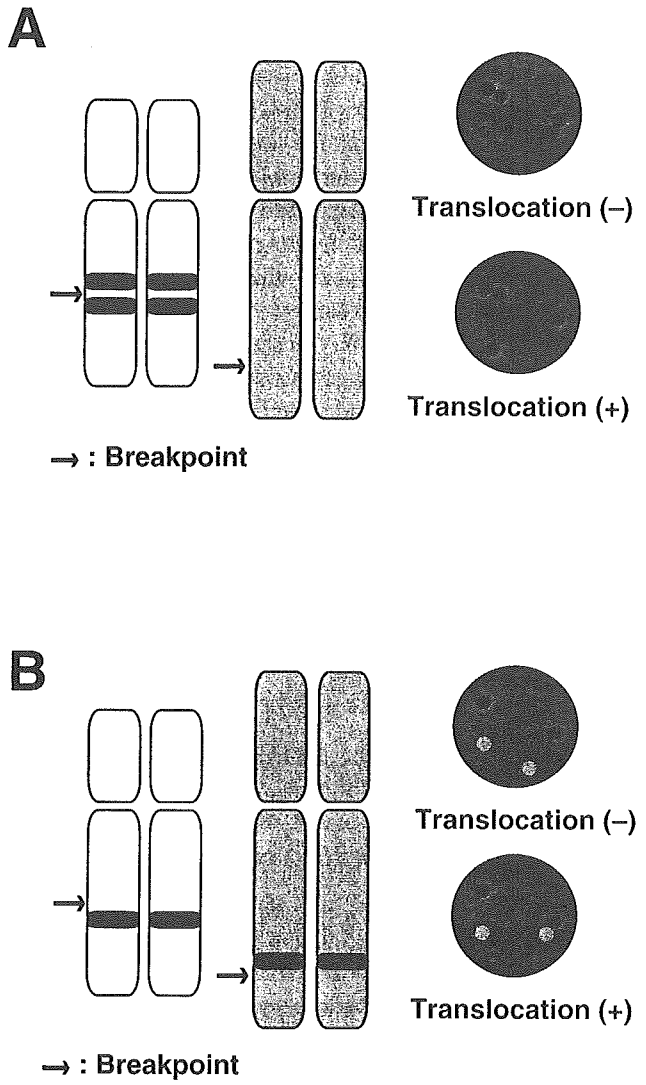

Fig. 2 Diagrammatic representation of intact and rearranged signals by specific gene probes in metaphase spread (left) and in interphase nuclei (right). (A) The two probes hybridize to genomic regions that are positioned on opposite sides from the breakpoint on a single translocated chromosome. (B) The two probes hybridize to regions on separate chromosomes.

for RT-PCR, we must completely avoid RNases. The following is the standard protocol for RNA extraction from paraffin sections.

Standard protocol of RNA extraction from paraffin sections

Five 10-μm-thick sections are cut from a representative paraffin block of each formalin-fixed tumor specimen and collected into a 1.5-mL tube. To avoid sample cross-contamination, a new microtome blade is used for each sample, and the area around the microtome is wiped frequently with 70% ethanol. Sterile forceps and new filter papers are used to transfer the each section. After deparaffinization with one xylene wash and two washes of absolute ethanol, the tissue sections are treated with 150 μL of lysis buffer (20 mM Tris-HCl, pH 8.0; 20 mM EDTA; and 2% SDS) and 5 μL of proteinase K (20 mg/mL). The samples are incubated 1 h at 55°C. After incubation, 450 μL of Trizol reagent (Gibco BRL, Gaithersburg, MD, USA) is added to the sample, and total RNA is extracted according to the manufacturer's instructions. RNA carriers, such as tRNA or glycogen, are required during the ethanol precipitation. The RNA pellet is resuspended in 10–20 μL of RNase-free water and subjected to deoxyribonuclease treatment. Five microliters of the DNase-treated RNA is promptly reverse-transcribed into cDNA using random primers.

CONCLUSION

Many types of sarcomas are characterized by specific chromosomal translocations resulting in the production of novel chimeric genes, and the discrete histopathological entities are remarkable. Sensitive molecular diagnostic assays classifying sarcomas have validated each other through a gratifying correlation of genotype and phenotype.

However, molecular targeting therapies using antibodies, RNA interference, and pharmacological inhibitors have arisen because these approaches are often effective. For example, gastrointestinal stromal tumors (GIST) are now defined as a specific, KIT-expressing, and KIT-signaling-driven mesenchymal tumor of the gastrointestinal tract. The specific identification of GIST has become more important since the availability of the KIT-selective tyrosine kinase inhibitor Imatinib mesylate, STI571, commercially known as Gleevec/Glivec (Novartis Pharma, Basel, Switzerland), for the treatment of unresectable and metastatic tumors. Many fusion proteins are believed to play key roles in the formation of each tumor type.[1,42] We do not yet have a therapeutic strategy for targeting fusion proteins. It was reported, however, that specific small interference RNA of EWS/FLI-1 resulted in complete growth arrest and increased the number of apoptotic cells dramatically.[43] Therefore, in the near future, it will be important to determine the genotypes of tumors not only for diagnosis, but also for molecular therapies.

REFERENCES

1. Barr FG. Translocations, cancer and the puzzle of specificity. *Nat Genet* 1998; **19**: 121–124.
2. Bennicelli JL, Barr FG. Genetics and the biologic basis of sarcomas. *Curr Opin Oncol* 1999; **11**: 267–274.
3. Ladanyi M, Bridge JA. Contribution of molecular genetic data to the classification of sarcomas. *Hum Pathol* 2000; **31**: 532–538.

4. Delattre O, Zucman J, Plougastel B *et al.* Gene fusion with an ETS DNA-binding domain caused by chromosome translocation in human tumours. *Nature* 1992; **359**: 162–165.
5. Zucman J, Melot T, Desmaze C *et al.* Combinatorial generation of variable fusion proteins in the Ewing family of tumours. *EMBO J* 1993; **12**: 4481–4487.
6. Sorensen PH, Lessnick SL, Lopez-Terrada D, Liu XF, Triche TJ, Denny CT. A second Ewing's sarcoma translocation, t(21;22), fuses the EWS gene to another ETS-family transcription factor, ERG. *Nat Genet* 1994; **6**: 146–151.
7. Jeon IS, Davis JN, Braun BS *et al.* A variant Ewing's sarcoma translocation (7;22) fuses the EWS gene to the ETS gene ETV1. *Oncogene* 1995; **10**: 1229–1234.
8. Kaneko Y, Yoshida K, Handa M *et al.* Fusion of an ETS-family gene, EIAF, to EWS by t (17;22) (q12;q12) chromosome translocation in an undifferentiated sarcoma of infancy. *Genes Chromosomes Cancer* 1996; **15**: 115–121.
9. Urano F, Umezawa A, Hong W, Kikuchi H, Hata J. A novel chimera gene between EWS and E1A-F, encoding the adenovirus E1A enhancer-binding protein, in extraosseous Ewing's sarcoma. *Biochem Biophys Res Commun* 1996; **219**: 608–612.
10. Peter M, Couturier J, Pacquement H *et al.* A new member of the ETS family fused to EWS in Ewing tumors. *Oncogene* 1997; **14**: 1159–1164.
11. Zucman J, Delattre O, Desmaze C *et al.* EWS and ATF-1 gene fusion induced by t(12;22) translocation in malignant melanoma of soft parts. *Nat Genet* 1993; **4**: 341–345.
12. Ladanyi M, Gerald W. Fusion of the EWS and WT1 genes in the desmoplastic small round cell tumor. *Cancer Res* 1994; **54**: 2837–2840.
13. Labelle Y, Zucman J, Stenman G *et al.* Oncogenic conversion of a novel orphan nuclear receptor by chromosome translocation. *Hum Mol Genet* 1995; **4**: 2219–2226.
14. Clark J, Benjamin H, Gill S *et al.* Fusion of the EWS gene to CHN, a member of the steroid/thyroid receptor gene superfamily, in a human myxoid chondrosarcoma. *Oncogene* 1996; **12**: 229–235.
15. Sjogren H, Meis-Kindblom J, Kindblom LG, Aman P, Stenman G. Fusion of the EWS-related gene TAF2N to TEC in extraskeletal myxoid chondrosarcoma. *Cancer Res* 1999; **59**: 5064–5067.
16. Panagopoulos I, Mencinger M, Dietrich CU *et al.* Fusion of the RBP56 and CHN genes in extraskeletal myxoid chondrosarcomas with translocation t(9;17)(q22;q11). *Oncogene* 1999; **18**: 7594–7598.
17. Attwooll C, Tariq M, Harris M, Coyne JD, Telford N, Varley JM. Identification of a novel fusion gene involving hTAFII68 and CHN from a t(9;17)(q22;q11.2) translocation in an extraskeletal myxoid chondrosarcoma. *Oncogene* 1999; **18**: 7599–7601.
18. Galili N, Davis RJ, Fredericks WJ *et al.* Fusion of a fork head domain gene to PAX3 in the solid tumour alveolar rhabdomyosarcoma. *Nat Genet* 1993; **5**: 230–235.
19. Shapiro DN, Sublett JE, Li B, Downing JR, Naeve CW. Fusion of PAX3 to a member of the forkhead family of transcription factors in human alveolar rhabdomyosarcoma. *Cancer Res* 1993; **53**: 5108–5112.
20. Davis RJ, D'Cruz CM, Lovell MA, Biegel JA, Barr FG. Fusion of PAX7 to FKHR by the variant t(1;13)(p36;q14) translocation in alveolar rhabdomyosarcoma. *Cancer Res* 1994; **54**: 2869–2872.
21. Crozat A, Aman P, Mandahl N, Ron D. Fusion of CHOP to a novel RNA-binding protein in human myxoid liposarcoma. *Nature* 1993; **363**: 640–644.
22. Rabbitts TH, Forster A, Larson R, Nathan P. Fusion of the dominant negative transcription regulator CHOP with a novel gene FUS by translocation t(12;16) in malignant liposarcoma. *Nat Genet* 1993; **4**: 175–180.
23. Panagopoulos I, Hoglund M, Mertens F, Mandahl N, Mitelman F, Aman P. Fusion of the EWS and CHOP genes in myxoid liposarcoma. *Oncogene* 1996; **12**: 489–494.
24. Clark J, Rocques PJ, Crew AJ *et al.* Identification of novel genes, SYT and SSX, involved in the t(X;18)(p11.2;q11.2) translocation found in human synovial sarcoma. *Nat Genet* 1994; **7**: 502–508.
25. Crew AJ, Clark J, Fisher C *et al.* Fusion of SYT to two genes, SSX1 and SSX2, encoding proteins with homology to the Kruppel-associated box in human synovial sarcoma. *EMBO J* 1995; **14**: 2333–2340.
26. de Leeuw B, Balemans M, Olde Weghuis D, Geurts van Kessel A. Identification of two alternative fusion genes, SYT-SSX1 and SYT-SSX2, in t(X;18) (p11.2;q11.2)-positive synovial sarcomas. *Hum Mol Genet* 1995; **4**: 1097–1099.
27. Skytting B, Nilsson G, Brodin B *et al.* A novel fusion gene, SYT-SSX4, in synovial sarcoma. *J Natl Cancer Inst* 1999; **91**: 974–975.
28. Simon MP, Pedeutour F, Sirvent N *et al.* Deregulation of the platelet-derived growth factor B-chain gene via fusion with collagen gene COL1A1 in dermatofibrosarcoma protuberans and giant-cell fibroblastoma. *Nat Genet* 1997; **15**: 95–98.
29. Knezevich SR, McFadden DE, Tao W, Lim JF, Sorensen PH. A novel ETV6-NTRK3 gene fusion in congenital fibrosarcoma. *Nat Genet* 1998; **18**: 184–187.
30. Thompson CT, LeBoit PE, Nederlof PM, Gray JW. Thick-section fluorescence *in situ* hybridization on

formalin-fixed, paraffin-embedded archival tissue provides a histogenetic profile. *Am J Pathol* 1994; **144**: 237–243.
31. Kuchinka BD, Kalousek DK, Lomax BL, Harrison KJ, Barrett IJ. Interphase cytogenetic analysis of single cell suspensions prepared from previously formalin-fixed and paraffin-embedded tissues. *Mod Pathol* 1995; **8**: 183–186.
32. Xiao S, Renshaw A, Cibas ES, Hudson TJ, Fletcher JA. Novel fluorescence *in situ* hybridization approaches in solid tumors. Characterization of frozen specimens, touch preparations, and cytological preparations. *Am J Pathol* 1995; **147**: 896–904.
33. Demetrick DJ. The use of archival frozen tumor tissue imprint specimens for fluorescence *in situ* hybridization. *Mod Pathol* 1996; **9**: 133–136.
34. Kumar S, Pack S, Kumar D *et al.* Detection of EWS-FLI-1 fusion in Ewing's sarcoma/peripheral primitive neuroectodermal tumor by fluorescence *in situ* hybridization using formalin-fixed paraffin-embedded tissue. *Hum Pathol* 1999; **30**: 324–330.
35. Monforte-Munoz H, Lopez-Terrada D, Affendie H, Rowland JM, Triche TJ. Documentation of EWS gene rearrangements by fluorescence *in-situ* hybridization (FISH) in frozen sections of Ewing's sarcoma-peripheral primitive neuroectodermal tumor. *Am J Surg Pathol* 1999; **23**: 309–315.
36. Birdsall S, Osin P, Lu YJ, Fisher C, Shipley J. Synovial sarcoma specific translocation associated with both epithelial and spindle cell components. *Int J Cancer* 1999; **82**: 605–608.
37. Qian X, Jin L, Shearer BM, Ketterling RP, Jalal SM, Lloyd RV. Molecular diagnosis of Ewing's sarcoma/primitive neuroectodermal tumor in formalin-fixed paraffin-embedded tissues by RT-PCR and fluorescence *in situ* hybridization. *Diagn Mol Pathol* 2005; **14**: 23–28.
38. Cremer T, Cremer C. Chromosome territories, nuclear architecture and gene regulation in mammalian cells. *Nat Rev Genet* 2001; **2**: 292–301.
39. Kuroda M, Tanabe H, Yoshida K *et al.* Alteration of chromosome positioning during adipocyte differentiation. *J Cell Sci* 2004; **117**: 5897–5903.
40. Kuroda M, Wang X, Sok J *et al.* Induction of a secreted protein by the myxoid liposarcoma oncogene. *Proc Natl Acad Sci USA* 1999; **96**: 5025–5030.
41. Kuroda M, Ishida T, Takanashi M, Satoh M, Machinami R, Watanabe T. Oncogenic transformation and inhibition of adipocytic conversion of preadipocytes by TLS/FUS-CHOP type II chimeric protein. *Am J Pathol* 1997; **151**: 735–744.
42. Cooper CS. Translocations in solid tumours. *Curr Opin Genet Dev* 1996; **6**: 71–75.
43. Prieur A, Tirode F, Cohen P, Delattre O. EWS/FLI-1 silencing and gene profiling of Ewing cells reveal downstream oncogenic pathways and a crucial role for repression of insulin-like growth factor binding protein 3. *Mol Cell Biol* 2004; **24**: 7275–7283.

Available online at www.sciencedirect.com
SCIENCE DIRECT®
Cancer Letters 228 (2005) 5–11
CANCER Letters
www.elsevier.com/locate/canlet

Mini-review

A review of DNA microarray analysis of human neuroblastomas

Miki Ohira[a], Shigeyuki Oba[b], Yoko Nakamura[a], Takahiro Hirata[c], Shin Ishii[b], Akira Nakagawara[a,*]

[a]*Division of Biochemistry, Chiba Cancer Center Research Institute, 666-2 Nitona, Chuoh-ku, Chiba 260-8717, Japan*
[b]*Graduate School of Information Science, Nara Institute of Science and Technology, Ikoma 630-0192, Japan*
[c]*Hisamitsu Pharmaceutical Co. Inc., Tokyo 100-622, Japan*

Received 20 December 2004; accepted 12 January 2005

Abstract

Neuroblastoma (NBL) is an enigmatic tumor with heterogeneous clinical behaviors including maturation, regression, and aggressive growth. Despite recent progress in therapeutic strategies against advanced NBL, long-term outcomes still remain very poor. The prediction of cancer prognosis is one of the most urgent demands to initiate the suitable treatment of NBL. Recent papers have demonstrated that cancers can be diagnosed on the basis of gene expression profiling. We have been proceeded NBL cDNA project to collect a large number of genes expressed in NBLs, to identify the genes differentially expressed between favorable and unfavorable NBLs, and to make an NBL-proper cDNA chip for large-scale analysis of NBL tumors. Computational analysis of gene expression data in NBLs identified many prognosis-related genes and provided a classifier to predict the patient prognosis with high efficiency. Conversion of these findings into better diagnosis and treatment is now underway. Thus, molecular profiling of NBL has become a feasible tool for clinical applications.

Keywords: Neuroblastoma; Expression profile; Microarray; Diagnosis; Prognosis prediction; Differential expression

1. Introduction

Neuroblastoma (NBL) is one of the most frequent solid cancers in young children and has variable clinical and biological characteristics [1]. Favorable type of tumors frequently regress spontaneously, while unfavorable type of tumors are often resistant to intensive chemotherapy and lead patients to fatal outcome. The poor prognosis of NBL patients depends on age at diagnosis (older than 12 months), advanced tumor stage (3 or 4), presence of *MYCN* amplification, low *TRKA* expression, unfavorable histology, diploidy, and chromosomal loss of 1p36 in tumors [2]. However, even these markers sometimes fail to classify the aggressiveness of tumors, especially for the intermediate type of NBL (stage 3 or 4 patients with single copy of *MYCN*). Moreover, some *MYCN*-amplified tumors can be distinguished by a better response to the combined treatment resulting in a better prognosis for

* Corresponding author. Tel.: +81 43 264 5431; fax: +81 43 265 1459.
E-mail address: akiranak@chiba-cc.jp (A. Nakagawara).

0304-3835/$ - see front matter © 2005 Elsevier Ireland Ltd. All rights reserved.
doi:10.1016/j.canlet.2005.01.054

Table 1
Genes whose expression is differential between neuroblastoma subsets and related to patient prognosis

Genes	Definition	Pattern[a]	Reference
TRKA	neurotrophic tyrosine kinase, receptor, type 1	F>UF	[3]
CD44	CD44 antigen	F>UF	[6]
PTN	Pleiotrophin	F>UF	[7]
CDC10	cell division cycle 10	F>UF	[10]
HRAS	v-Ha-ras Harvey rat sarcoma viral oncogene	F>UF	[9]
XCE	endothelin-converting enzyme-like 1	F>UF	[17]
NLRR3	neuronal leucine-rich repeat 3	F>UF	[18]
TTL	tubulin tyrosine ligase	F>UF	[19]
BMCC1	novel putative apoptosis-related gene with BCH domain	F>UF	
FOG2	Friend of GATA protein 2	F>UF	[16]
NEDL1	NEDD4-like ubiquitin ligase 1	F>UF	
NEDL2	NEDD4-like ubiquitin ligase 2	F>UF	
GABARAP	gamma-aminobutyric acid receptor-associated protein gene	F>UF	[20]
GABA(A) family	GABA(A) receptor subunit gene family	F>UF	[20]
TRKB	neurotrophic tyrosine kinase, receptor, type 2	F<UF	[4]
hTERT	telomerase reverse transcriptase	F<UF	[5]
NM23A	non-metastatic cells 1 (*NM23-H1*)	F<UF	[12]
NM23B	non-metastatic cells 2 (*NM23-H2*)	F<UF	[13]
BIRC5	baculoviral IAP repeat-containing 5 (survivin)	F<UF	[11]
PPM1D	protein phosphatase 1D	F<UF	[14]
NLRR1	neuronal leucine-rich repeat 1	F<UF	[18]
LMO3	LIM-only protein 3	F<UF	

[a] F;favorable NBL, UF;unfavorable NBL.

the patient. Therefore, additional potent markers for predicting the NBL prognosis should be discovered to construct a more effective as well as less toxic therapeutic strategy. Recent works have demonstrated that cancers can be diagnosed on the basis of gene expression profiling using cDNA microarrays with calculation by computational algorithms. This process needs (1) mass collection or identification of genes expressed in NBLs, (2) construction of a DNA chip and analysis of tumor samples, (3) computational analysis of gene expression data and identification of prognosis-related genes, and (4) conversion of these findings into better diagnosis and treatment. In this review, we discuss the recent attempts of large-scale molecular profiling of NBL and their future applications to the clinic.

2. Prognostic markers for neuroblastoma

In addition to conventional prognostic markers such as age, INSS stage, *MYCN* copy number, histology, and DNA ploidy, expression levels of several genes have recently been added as new indicators. They include inverse relationship of *TRKA* and *TRKB* expression [3,4], *telomerase* [5], *CD44* [6], *pleiotrophin* [7], *N-cadherin* [8], *H-RAS* [9], and *CDC10* [10] (Table 1). From the analyses of genomic aberrations occurred in NBLs, several candidate genes that exhibit overexpression in advanced NBL were identified such as *survivin* [11], *NM23-H1* and *NM23-H2* [12,13], and *PPM1D* [14]. These genes are located on chromosome 17q, which is known to be frequently increased chromosomal copies in advanced NBLs.

3. Identification of novel prognosis-related genes

Various genomic approaches have been used to identify differentially expressed genes among different tissue and tumor types, including differential hybridization screening, representational difference analysis (RDA), gene counting using cDNA libraries followed by semi-quantitative reverse transcriptase polymerase chain reaction (RT-PCR) screening, serial analysis of

gene expression (SAGE), suppression subtractive hybridization (SSH), and cDNA and oligonucleotide microarrays.

In order to collect a large number of genes expressed in various type of NBLs, we have constructed oligo-capping cDNA libraries from primary NBL tissues with different biological characteristics: the tumors with favorable (F; stage 1, single copy of *MYCN*, high *TrkA* expression) and unfavorable (UF; stage 3 or 4, amplification of *MYCN*, no expression of *TrkA*) characteristics and the stage 4 S tumor [15,16]. Ten thousands of clones in total were isolated from those libraries, which corresponded 5,340 independent genes, and approximately 40% of those were shown to contain novel sequences by database search [16]. To identify the genes expressed differentially between the F and UF subsets, all independent clones except housekeeping genes were subjected to semi-quantitative RT-PCR analysis using RNAs obtained from 16 F and 16 UF NBL tissues as templates. From this project, we have identified more than 500 genes differentially expressed between F and UF NBLs. These included many novel genes with unknown functions, including endothelin-converting enzyme-like 1 (*XCE/ECEL1*) [17], neuronal leucine-rich repeat family members (*NLRR1* and *NLRR3*) [18], tubulin tyrosine ligase (*TTL*) [19], novel putative apoptosis-related gene with BCH domain (*BMCC1*, Machida et al., manuscript in preparation), a member of LIM-only protein (*LMO3*) (Aoyama et al., under submission), and NEDD4-like ubiquitin E3 ligase (*NEDL1* and *NEDL2*) (Miyazaki et al., manuscript in preparation) (Table 1). All these genes were analyzed by quantitative real-time RT-PCR method and confirmed to be strongly related to patient prognosis of NBLs. These genes are now being investigated by functional analysis.

Roberts et al. [20] have applied SSH technique to identify potential NBL biomarkers that may improve outcome prediction, and identified differential expression of members of the GABAergic gene family in NBL. They found that low levels of gamma-aminobutyric acid (GABA) receptor-associated protein (*GABARAP*) gene expression predict decreased survival, and that GABA(A) delta receptor subunit gene expression was predictive of a poor outcome among stage 4S patients.

4. Expression profiling of neuroblastomas by microarray approach

Recently, the DNA microarray method has been applied to comprehensively demonstrate the expression profiles of primary NBLs and cell lines (Table 2). The first microarray-based gene expression profiling study of NBL was reported by Khan et al. [21], who demonstrated that the small, round blue-cell tumors (SRBCTs), including NBL, rhabdomyosarcoma, non-Hodgkin lymphoma, and the Ewing family of tumors, which is often present diagnostic dilemmas in clinical practice, could be distinguished on the basis of their patterns of gene expression using artificial neural networks (ANNs). Among these SRBCTs, they showed that 6 of 7 test samples with NBL were classified correctly by using 93 unique genes. Among the 93 classifier genes, 15 genes were highly and specifically expressed in NBLs. This finding is very important when diagnostic tool is going to apply the gene expression data, because it is the first point to be confirmed whether the tumor, which is to be examined, is NBL or not.

Subsequent microarray studies have facilitated class separation of differentiating NBL tumors from poorly differentiated tumors and of high-risk tumors from low-risk tumors. Yamanaka et al. [22] examined 14 NBLs by 23,040 cDNAs microarray, and identified 78 genes whose expression levels were significantly different between differentiating NBLs and poorly differentiated NBLs. The 78 genes included those associated with cell maturation and apoptosis; 15 genes that were up-regulated in stage 4 tumors included those encoding cell adhesion molecules and cytoskeleton proteins. Berwanger et al. [23] examined expression profiles from 94 primary NBL specimens using a 4,608 cDNA human unigene chip. They found 24 significant genes differentially expressed between stage 1 ($n=19$) and stage 4 ($n=21$) *MYCN* non-amplified tumors. Interestingly, a significant percentage of the 24 genes encoded those involved in signaling through the nonreceptor tyrosine kinase Fyn and the actin cytoskeleton. These genes were coordinately down-regulated in advanced stage NBL, both in *MYCN* amplified and nonamplified tumors (Table 2). They also showed that expression of *FYN* predicts long term survival of NBL patients, independently of *MYCN* amplification. Takita et al. [24] performed DNA microarray analysis on 20

Table 2
Differentially expressed genes identified by gene expression profiling using microarray

	Genes identified	Genes on microarray	Sample number	Category
NBL diagnosis				
Khan et al. [21]	15 genes	6,567cDNAs	16 NBLs	For SRBCTs diagnosis *DPYSL4, CDH2, AF1Q, CRMP1, KIF3C, GAP43, MAP1B, RCV1, SFRP1, GATA2, PFN2, FHL1* (highly and specifically expressed in NBLs)
Expression profiling				
Yamanaka et al. [22]	78 genes	23,040 cDNAs	14 NBLs	Differentiating NBLs vs. poorly differentiated NBLs *ITGE, SYP, OLIG2, MADH2, DFFB, CASP8, CASP9* (up-regulated in differentiating NBLs) *CLDN5, CCND1, NFKBIL2* (up-regulated in poorly differentiated NBLs)
Berwanger et al. [23]	36 genes	4,608 cDNAs	94 NBLs	Stage 1 vs. stage 4 *MYCN* non-amplified tumors *FYN, AFAP, CTNNA1, NRCAM, tropomodulin, MARCKS* (down-regulated in advanced stage NBL)
Takita et al. [24]	3 genes	1,700 genes	20 NBLs	Stage 1 vs. stage 4 *BIRC3, CDKN2D* (up-regulated in the early-stage group) *SMARCD3* (down-regulated in the early-stage group)
Hiyama et al. [25]	123 genes	6,272 cDNAs	20 NBLs	Unfavorable vs. favorable (regressing and maturing) 43 genes including *MYCN, hTERT, NME1, CCND1, CCNE1, E1, BIRC5, BIRC1* (up-regulated in unfavorable NBLs) 80 genes (up-regulated in favorable NBLs) *CD44, IGF2, TRKA, ANK1* (highly expressed in maturing NBLs) *CASP8, CASP9, TNFSF10, NGFA, GDF10* (highly expressed in regressing NBLs)
McArdle et al. [26]		14,500 genes	20 NBLs	Differentially expressed in the 11q-, MYCN non-amplified and hyperdiploid subtypes of NBL
Janoueix-Lerosey et al.[27]		320 genes (on 1p35-36)	43 NBLs	1p loss vs. 1p-normal *CDC42, VAMP3, CLSTN1, GNB1, STMN1, RPA2, RBAF600, FBXO6, MAD2L2* (decreased expression in NBLs with 1p deletion)
Prognosis prediction				
Wei et al. [28]	19 genes	42,578 cDNA	56 NBLs	To develop an accurate predictor of survival for patient with NBL *DLK1, PRSS3, ARC, SLIT3, MYCN, JPH1* (up-regulated in the poor-outcome group) *ARHI, CNR1, CD44, ROBO2, BTBD3, KLRC3* (down-regulated in the poor-outcome group)
Ohira et al. [29]	70 genes	5,340 cDNAs	136 NBLs	To develop an accurate predictor of survival for patient with NBL

primary tumors (stage 1 versus 4) and identified that the expression of *BIRC3* and *CDKN2D* genes were significantly higher in the early-stage group than in the advanced-stage group and that the expression of the *SMARCD3* gene was significantly reduced in the early-stage group. The *BIRC3*, *CDKN2D*, and *SMARCD3* genes have been reported to be associated with apoptosis, cell cycles, and the transcriptional activator, respectively. Hiyama et al. [25] analyzed 20 NBLs with 6272 cDNAs microarray, and revealed that 43 genes, including *MYCN*, *hTERT*, *NM23-H1*, cell cycle regulatory protein-coding genes (*CCND1*, *CCNE1*, *E1*), and apoptosis-escape genes (*BIRC5*, *BIRC1*) were highly expressed in unfavorable neuroblastomas, while another 80 genes, including neuronal differentiating genes and apoptotic inducing genes (*CD44*, *IGF2*, *TRKA*, *ANK1* in maturing NBLs, *CASP8*, *CASP9*, *TNFSF10*, *NGFA*, *GDF10* in regressing NBLs) were detected as highly expressed in favorable tumors.

There have been several studies by focusing the certain genomic aberrations and corresponding gene expression profiles. McArdle et al. [26] identified transcripts that are differentially expressed in the 11q-, *MYCN* nonamplified and hyperdiploid subtypes of NBL. Janoueix-Lerosey et al. [27] compared the expression profiles between the tumors with 1p loss and those with normal 1p status and identified the genes with decreased expression in NBLs with 1p deletion (Table 2).

5. Microarray-based system for predicting prognosis of neuroblastoma patients

We now have in our hands the increasing number of information for genes which can distinguish prognosis of the patient with NBL as described above. These data should subsequently be integrated and organized to construct a simple prediction system which is practical for the clinic. Such efforts are now ongoing.

Wei et al. [28] have performed gene expression profiling of 56 NBLs using cDNA microarrays containing 42,578 cDNA clones and used artificial neural networks (ANNs) to develop an accurate predictor of survival for each individual patient with NBL. ANN-based prognosis prediction has been accomplished by using expression levels of only 19 genes including *MYCN* and *CD44*. In addition, these 19 predictor genes were able to additionally classify high-risk patients into two subgroups according to their survival status. Among these predictor genes, *DLK1*, *PRSS3*, *ARC*, *SLIT3*, *MYCN* and *JPH1* were up-regulated in the poor-outcome group included, whereas *ARHI*, *CNR1*, *CD44*, *ROBO2*, *BTBD3* and *KLRC3* were down-regulated.

We also have constructed an in-house, microceramic pump-based ink-jet-printed cDNA microarray carrying 5,340 genes obtained from primary NBL cDNA libraries and applied it for the analysis of 136 tumors. A probabilistic output computational analysis using learning samples has selected 70 genes which constructed a classifier for patient outcome, and provided a correct prognosis of test samples with high efficiency [29]. Of clinical interest, Kaplan-Meier analysis indicated that the classifier can divide significantly 5-year survivals of NBL patients, even for the intermediate risk type. Furthermore, our microarray prediction exhibited the best balance between sensitivity and specificity among prognostic factors including *MYCN* amplification and *TrkA* expression.

These findings provide evidence of a gene expression signature that can predict prognosis independent of currently known risk factors and could assist physicians in the individual management of patients with high-risk NBL. Such gene expression-based diagnosis system should be highly accurate and reproducible, as well as simple, easy to analyze, and with low cost. Based on this, we subsequently made a mini-chip carrying top-ranked 200 genes for clinical use. We are now investigating its (1) reproducibility from the original 5,340 genes chip, (2) potential of predicting prognosis for the newly added test samples, (3) potential of predicting prognosis when whole experimental process (RNA isolation, sample labeling, hybridization, and calculation of the probability of patient survival by using the classifier) is conducted in an independent laboratory. After confirming these, the microarray system will come to prove its practical use to be feasible in the clinic to predict the prognosis of the patient with NBL.

6. Conclusion

Using the gene expression profiling, we are now able to distinguish a group of high-risk patients with high efficiency who will not respond to conventional therapy and therefore require alternative treatment strategies. Although further prospective studies will be necessary, we may also be able to reduce the toxicity of treatment regime for the patients who have been predicted to survive according to gene expression profile. Recently, in addition to the gene expression profiling, certain genome aberrations as well as epigenetic alterations have been reported to be strongly related to the patient prognosis with NBL. Abe et al. [30] indicated that poor NBLs suffer the increased methylation pressure in their tumor genome, and that the methylation of certain CpG island, such as *Protocadherin beta* family, can predict poor NBL prognosis with high sensitivity. Furthermore, screening of prognosis-related proteins secreted into serum of NBL patients has been started by many groups. Combination of such independent systems to predict

prognosis will further improve the accuracy of the diagnostic system for NBL.

Acknowledgements

This work was supported in part by a fund from Hisamitsu Pharmaceutical Co., Inc. and by Grant-in-Aids for Scientific Research on Priority Areas (C) 'Medical Genome Science' and 'Genome Information Science', and for Scientific Research (B) from the Ministry of Education, Culture, Sports, Science and Technology of Japan, and by Grant-in Aids for Cancer Research and for the 2nd Term Comprehensive 10-year Strategy for Cancer Control from the Ministry of Health, Labour and Welfare of Japan.

References

[1] R.P. Bolande, The neurocristopathies: a unifying concept of disease arising in neural crest maldevelopment, Hum. Pathol. 5 (1974) 409–429.

[2] J.L. Weinstein, H.M. Katzenstein, S.L. Cohn, Advances in the diagnosis and treatment of neuroblastoma, Oncologist 8 (2003) 278–292.

[3] A. Nakagawara, M. Arima-Nakagawara, N.J. Scavarda, C.G. Azar, A.B. Cantor, G.M. Brodeur, Association between high levels of expression of the TRK gene and favorable outcome in human neuroblastoma, N. Engl. J. Med. 328 (1993) 847–854.

[4] A. Nakagawara, C.G. Azar, N.J. Scavarda, G.M. Brodeur, Expression and function of TRK-B and BDNF in human neuroblastomas, Mol. Cell Biol. 14 (1994) 759–767.

[5] E. Hiyama, K. Hiyama, T. Yokoyama, Y. Matsuura, M.A. Piatyszek, J.W. Shay, Correlating telomerase activity levels with human neuroblastoma outcomes, Nat. Med. 1 (1995) 249–255.

[6] M.C. Favrot, V. Combaret, C. Lasset, CD44–a new prognostic marker for neuroblastoma, N. Engl. J. Med. 1993; 329.

[7] A. Nakagawara, J. Milbrandt, T. Muramatsu, T.F. Deuel, H. Zhao, A. Cnaan, G.M. Brodeur, Differential expression of pleiotrophin and midkine in advanced neuroblastomas, Cancer Res. 55 (1995) 1792–1797.

[8] R. Shimono, S. Matsubara, H. Takamatsu, T. Fukushige, M. Ozawa, The expression of cadherins in human neuroblastoma cell lines and clinical tumors, Anticancer Res. 20 (2000) 917–923.

[9] T. Tanaka, T. Sugimoto, T. Sawada, Prognostic discrimination among neuroblastomas according to Ha-ras/trk A gene expression: a comparison of the profiles of neuroblastomas detected clinically and those detected through mass screening, Cancer 83 (1998) 1626–1633.

[10] T. Nagata, Y. Takahashi, S. Asai, Y. Ishii, H. Mugishima, T. Suzuki, et al., The high level of hCDC10 gene expression in neuroblastoma may be associated with favorable characteristics of the tumor, J. Surg. Res. 92 (2000) 267–275.

[11] A. Islam, H. Kageyama, N. Takada, T. Kawamoto, H. Takayasu, E. Isogai, et al., High expression of Survivin, mapped to 17q25, is significantly associated with poor prognostic factors and promotes cell survival in human neuroblastoma, Oncogene 19 (2000) 617–623.

[12] N. Hailat, D.R. Keim, R.F. Melhem, X.X. Zhu, C. Eckerskorn, G.M. Brodeur, et al., High levels of p19/nm23 protein in neuroblastoma are associated with advanced stage disease and with N-myc gene amplification, J. Clin. Invest. 88 (1991) 341–345.

[13] A. Leone, R.C. Seeger, C.M. Hong, Y.Y. Hu, M.J. Arboleda, G.M. Brodeur, et al., Evidence for nm23 RNA overexpression, DNA amplification and mutation in aggressive childhood neuroblastomas, Oncogene 8 (1993) 855–865.

[14] F. Saito-Ohara, I. Imoto, J. Inoue, H. Hosoi, A. Nakagawara, T. Sugimoto, J. Inazawa, PPM1D is a potential target for 17q gain in neuroblastoma, Cancer Res. 63 (2003) 1876–1883.

[15] M. Ohira, A. Morohashi, Y. Nakamura, E. Isogai, K. Furuya, S. Hamano, et al., Neuroblastoma oligo-capping cDNA project: toward the understanding of the genesis and biology of neuroblastoma, Cancer Lett. 197 (2003) 63–68.

[16] M. Ohira, A. Morohashi, H. Inuzuka, T. Shishikura, T. Kawamoto, H. Kageyama, et al., Expression profiling and characterization of 4200 genes cloned from primary neuroblastomas: identification of 305 genes differentially expressed between favorable and unfavorable subsets, Oncogene 22 (2003) 5525–5536.

[17] T. Kawamoto, M. Ohira, S. Hamano, T. Hori, A. Nakagawara, High expression of the novel endothelin-converting enzyme genes, Nbla03145/ECEL1alpha and beta, is associated with favorable prognosis in human neuroblastomas, Int. J. Oncol. 22 (2003) 815–822.

[18] S. Hamano, M. Ohira, E. Isogai, K. Nakada, A. Nakagawara, Identification of novel human neuronal leucine-rich repeat (hNLRR) family genes and inverse association of expression of Nbla10449/hNLRR-1 and Nbla10677/hNLRR-3 with the prognosis of primary neuroblastomas, Int. J. Oncol. 24 (2004) 1457–1466.

[19] C. Kato, K. Miyazaki, A. Nakagawa, M. Ohira, Y. Nakamura, T. Ozaki, et al., Low expression of human tubulin tyrosine ligase and suppressed tubulin tyrosination/detyrosination cycle are associated with impaired neuronal differentiation in neuroblastomas with poor prognosis, Int. J. Cancer 112 (2004) 365–375.

[20] S.S. Roberts, M. Mori, P. Pattee, J. Lapidus, R. Mathews, J.P. O'Malley, et al., GABAergic system gene expression predicts clinical outcome in patients with neuroblastoma, J. Clin. Oncol. 22 (2004) 4127–4134.

[21] J. Khan, J.S. Wei, M. Ringner, L.H. Saal, M. Ladanyi, F. Westermann, et al., Classification and diagnostic prediction of cancers using gene expression profiling and artificial neural networks, Nat. Med. 7 (2001) 673–679.
[22] Y. Yamanaka, Y. Hamazaki, Y. Sato, K. Ito, K. Watanabe, T. Heike, et al., Maturational sequence of neuroblastoma revealed by molecular analysis on cDNA microarrays, Int. J. Oncol. 21 (2002) 803–807.
[23] B. Berwanger, O. Hartmann, E. Bergmann, S. Bernard, D. Nielsen, M. Krause, et al., Loss of a FYN-regulated differentiation and growth arrest pathway in advanced stage neuroblastoma, Cancer Cell 2 (2002) 377–386.
[24] J. Takita, M. Ishii, S. Tsutsumi, Y. Tanaka, K. Kato, Y. Toyoda, et al., Gene expression profiling and identification of novel prognostic marker genes in neuroblastoma, Genes Chromosomes Cancer 40 (2004) 120–132.
[25] E. Hiyama, K. Hiyama, H. Yamaoka, T. Sueda, C.P. Reynolds, T. Yokoyama, Expression profiling of favorable and unfavorable neuroblastomas, Pediatr. Surg. Int. 20 (2004) 33–38.
[26] L. McArdle, M. McDermott, R. Purcell, D. Grehan, A. O'Meara, F. Breatnach, et al., Oligonucleotide microarray analysis of gene expression in neuroblastoma displaying loss of chromosome 11q, Carcinogenesis 25 (2004) 1599–1609.
[27] I. Janoueix-Lerosey, E. Novikov, M. Monteiro, N. Gruel, G. Schleiermacher, B. Loriod, et al., Gene expression profiling of 1p35-36 genes in neuroblastoma, Oncogene 23 (2004) 5912–5922.
[28] J.S. Wei, B.T. Greer, F. Westermann, S.M. Steinberg, C.G. Son, Q.R. Chen, et al., Prediction of clinical outcome using gene expression profiling and artificial neural networks for patients with neuroblastoma, Cancer Res. 64 (2004) 6883–6891.
[29] M. Ohira, S. Oba, Y. Nakamura, E. Isogai, S. Kaneko, A. Nakagawa, et al., Expression profiling using a tumor-specific cDNA microarray prediols the prognosis of intermediate-risk neuroblastomas, Cancer Cell 7 (2005) 337-350.
[30] M. Abe, M. Ohira, A. Kaneda, Y. Yagi, S. Yamamoto, Y. Kitano, et al., CpG island methylator phenotype is a strong determinant of poor prognosis in neuroblastomas, Cancer Res., 65 (2005) 828–834.

Expression profiling using a tumor-specific cDNA microarray predicts the prognosis of intermediate risk neuroblastomas

Miki Ohira,[1,8] Shigeyuki Oba,[2,8] Yohko Nakamura,[1] Eriko Isogai,[1] Setsuko Kaneko,[3] Atsuko Nakagawa,[4] Takahiro Hirata,[5] Hiroyuki Kubo,[5] Takeshi Goto,[5] Saichi Yamada,[6] Yasuko Yoshida,[6] Misa Fuchioka,[7] Shin Ishii,[2] and Akira Nakagawara[1,*]

[1]Division of Biochemistry, Chiba Cancer Center Research Institute, Chiba 260-8717, Japan
[2]Graduate School of Information Science, Nara Institute of Science and Technology, Ikoma 630-0192, Japan
[3]Department of Pediatric Surgery, University of Tsukuba School of Medicine, Tsukuba 305-8575, Japan
[4]Second Department of Pathology, Aichi Medical University, Nagakute 480-1195, Japan
[5]Hisamitsu Pharmaceutical Co. Inc., Tokyo 100-622, Japan
[6]Micro Ceramics Laboratory, R & D Center, NGK Insulators, LTD, Nagoya 467-8530, Japan
[7]Center for Molecular Biology and Cytogenetics SRL Inc., Tokyo 191-0002, Japan
[8]These authors contributed equally to this work.
*Correspondence: akiranak@chiba-cc.jp

Summary

To predict the prognosis of neuroblastoma patients and choose a better therapeutic protocol, we developed a cDNA microarray carrying 5340 genes obtained from primary neuroblastomas and examined 136 tumor samples. We made a probabilistic output statistical classifier that provided a high accuracy in prognosis prediction (89% at 5 years) and a highly reliable method to validate it. Kaplan-Meier analysis indicated that the patients in an intermediate group defined by existing markers are divided by microarray into two further groups with 5 year survivals for 36% and 89% of patients ($p < 10^{-4}$), i.e., with unfavorably and favorably predicted neuroblastomas, respectively. According to these results, we developed a gene subset chip for a clinical tool, for which our classifier exhibited 88% prediction accuracy.

Introduction

Neuroblastoma is one of the most common solid tumors in children and originates from the sympathoadrenal lineage of the neural crest (Bolande, 1974). Its clinical behaviors are heterogeneous. The tumor, when developed in infants, frequently regresses spontaneously by inducing differentiation and/or programmed cell death. When developed in children over 1 year of age, however, the tumor is often aggressive and acquires resistance to intensive chemotherapy. Although recent progress in therapeutic strategies against advanced neuroblastoma has improved patient survival, long-term outcomes still remain very poor. Furthermore, part of neuroblastomas categorized to the intermediate group (stage 3 or 4 tumors that possess a single copy of the *MYCN* gene) often recurs after complete response to initial therapy. Such differences in the final outcomes of the tumor are considered presumably attributable to differences in genetic and biological abnormalities, which are reflected in the gene and protein expression profiles of the tumor.

The prediction of cancer prognosis is one of the most urgent demands to initiate the treatment of neuroblastoma. As expected from the natural course of neuroblastoma, patient age at diagnosis (over or under 1 year of age) is an important prognostic factor (Evans et al., 1971). Disease stage is also a powerful indicator for neuroblastoma prognosis (Brodeur et al., 1993). Moreover, recent advances in basic research have discovered several molecular markers that are useful in clinical practice, including amplification of the *MYCN* oncogene (Schwab et al., 1983; Brodeur et al., 1984), DNA ploidy (Look et al., 1984; Look et al., 1991), deletion of chromosome 1p (Brodeur et al., 1988), and *TrkA* expression (Nakagawara et al., 1992; Nakagawara et al., 1993). Other indicators also include *telomerase* (Hiyama et al., 1995), *CD44* (Favrot et al., 1993), *pleiotrophin* (Nakagawara et al., 1995), *N-cadherin* (Shimono et al., 2000), *CDC10* (Nagata et al., 2000), and *Fyn* (Berwanger et al., 2002). However, the combinations thereof still frequently fail to predict patient outcome. In the post-genome sequence era, therefore, the advent of new diagnostic tools has been ex-

SIGNIFICANCE

Neuroblastoma is an enigmatic tumor with heterogeneous clinical behaviors including maturation, regression, and growth. Despite recent improvements in the cure rate of many pediatric tumors, the prognosis of advanced neuroblastoma is still poor. In addition, it is usually difficult to predict the prognosis of the intermediate risk group in advanced stages without *MYCN* amplification. Through our supervised machine learning and highly reliable statistical validation procedure with the 5 year prognosis of the patients, we established a simple, low-cost microarray system carrying top-ranked genes, which exhibited high accuracy (88%) to predict the neuroblastoma prognosis and is highly feasible as a clinical tool.

pected. Recently, the DNA microarray method, applied to comprehensively demonstrate expression profiles of primary neuroblastomas and cell lines, has already identified the following: (1) differences in gene expression between favorable and unfavorable subsets (Yamanaka et al., 2002; Berwanger et al., 2002); and (2) differences in gene expression that occur during retinoic acid-induced neuronal differentiation (Ueda, 2001). However, a study to predict neuroblastoma prognosis with a microarray using a large number of neuroblastoma samples has never been reported. We have recently isolated 5500 genes from the cDNA libraries, which were generated from primary neuroblastomas, part of which has previously been reported (Ohira et al., 2003a; Ohira et al., 2003b). In this study, to identify genes strongly associated with neuroblastoma prognosis and to apply them to make a really practical cDNA microarray for neuroblastoma diagnosis, we constructed an in-house, ink-jet-printed cDNA microarray carrying 5340 genes proper to neuroblastoma and applied it to analyze 136 samples. After selecting genes significantly related to patient prognosis, we made a mini-chip carrying 200 top-ranked genes to apply for the clinic.

There have been many attempts to predict cancer outcome using microarray. A reliable prediction for outcomes of cancer patients naturally demands its reproducibility, and it is quite important to use sound and highly reliable statistical methodologies; a complete crossvalidation analysis without introducing any information leakage and an independent test using new samples are necessary. As Ntzani and Ioannidis (2003) pointed out, however, such a careful methodology has often been ignored in most microarray studies. We here developed a supervised classification method without any information leakage as a statistic tool and demonstrated that the probabilistic output of the analysis defines the molecular signature of neuroblastoma to predict its prognosis. Although the construction of the statistical tool was based on one of the most reliable statistical tests, we also consulted a validation test for an independent experiment examining 50 samples (whose RNAs were prepared in an independent laboratory) by using the mini-chip. The high performance for the outcome prediction by the mini-chip system suggests the high feasibility of developing a clinical tool based on molecular signature.

Results

Neuroblastoma proper cDNA microarray

The whole scheme of our study is summarized in Figure 1. We first constructed a neuroblastoma proper cDNA microarray harboring the spots of 5340 genes on a slide glass by using a ceramics-based ink-jet printing system (the 5340 genes system). This in-house cDNA microarray appeared to have overcome the previous problems caused by pin-spotting, e.g., uneven quantity or shape of individual spots on an array. Ten micrograms each of the total RNA extracted from 136 frozen tissues of primary neuroblastomas were labeled with Cy3 dye. As a common reference, the mixture of the total RNA obtained from four neuroblastoma cell lines with a single copy of *MYCN* (NB69, NBLS, SK-N-AS, and SH-SY5Y) was labeled with Cy5 dye.

We first evaluated the quality of our cDNA microarray, the 5340 genes system. The log Cy3/Cy5 fluorescence ratio of each gene spot was normalized to eliminate intensity-dependent biases. Since the 5340 genes array contains 260 duplicated or multiplicated genes, the expression ratio of such a duplicated gene was represented by the average of multiple spots. Based on estimation performance for missing values (see the Supplemental Data available with this article online) and on reproduction variance of the duplicated genes, the standard deviation for the log ratio of a single gene was sufficiently small, ranging between about 0.2 and about 0.3 (Figure S1A). The scatter plots of the log Cy3/Cy5 fluorescence ratio between duplicated gene spots in the 136 experiments and those between repeated experiments also indicated high reproducibility of spotting and experiment (Figures S1B and S1C). These suggest that the production of and experiments by our cDNA microarray are highly reproducible.

Supervised classification

To develop a statistical tool that predicts the prognosis of a new patient with neuroblastoma, we introduced a supervised classification. In the development, we used 136 neuroblastomas, randomly selected tumor samples from the neuroblastoma tissue bank, consisting of 41 stage 1 tumors, 22 stage 2 tumors, 33 stage 3 tumors, 28 stage 4 tumors, and 12 stage 4s tumors. The follow-up duration ranged between 3 and 241 months (median, 56 months, mean, 57.3 months) after diagnosis. The left panel in Figure 2 compiles summary information of each sample, including survival time and important prognosis markers (see Experimental Procedures for details). Since variations in follow-up duration generated noises in the supervised classification, we used patient outcome (dead or alive) at 5 years after diagnosis as the target label to be predicted. Since the outcomes of 40 of 136 samples were unknown at 5 years after diagnosis, data for 96 remaining samples were used subsequently. When we were interested in short-term outcome prediction, the target label was set at 2 years after diagnosis, for which purpose 126 samples out of the 136 samples were used.

We constructed the weighted voting as a supervised classifier after important genes were selected according to pairwise *F* scores. To estimate the prediction accuracy for new data, we consulted leave two out (LTO) analysis, which obtains almost unbiased estimation of prediction accuracy for new data while avoiding overestimation due to information leakage (Figure S2A). Although it is known that the prediction accuracy of a supervised classifier depends on the number of genes to be used (Figure S3), the LTO procedure enables us to optimize it without introducing information leakage, by using a sample left out at the outer loop of the double-loop procedure (see Experimental Procedures). The crossvalidation accuracy for the 5 year prognosis prediction was as high as 88.5% (sensitivity of 86.7% and specificity of 89.4%) (Table 1, "Whole cases"). In the LTO analysis, we selected genes and constructed the corresponding classifier individually for the outcome prediction of each sample. The average number of the selected genes, n, was 30.7. If we applied the same procedure to the short-term (2 year) prediction, the accuracy, sensitivity, and specificity were 89.8%, 88.0%, and 90.2%, respectively (data not shown).

Construction of a probabilistic output

According to the LTO analysis, we can obtain weighted vote values and the corresponding survival rates. After approximat-